

## University of Wollongong Research Online

---

Faculty of Engineering - Papers (Archive)

Faculty of Engineering and Information  
Sciences

---

2010

### Potential high resolution dosimeters for MRT

E. Brauer-Krisch

*European Synchrotron Radiation Facility (ESRF)*

Anatoly B. Rosenfeld

*University of Wollongong, anatoly@uow.edu.au*

Michael L. Lerch

*University of Wollongong, mlerch@uow.edu.au*

Marco Petasecca

*University of Wollongong, marcop@uow.edu.au*

M. Akselrod

*Stillwater Crystal Growth Division USA*

*See next page for additional authors*

Follow this and additional works at: <https://ro.uow.edu.au/engpapers>



Part of the [Engineering Commons](#)

<https://ro.uow.edu.au/engpapers/4291>

---

#### Recommended Citation

Brauer-Krisch, E.; Rosenfeld, Anatoly B.; Lerch, Michael L.; Petasecca, Marco; Akselrod, M.; Sykora, J.; Bartz, J.; Ptaszkiewicz, M.; Olko, P.; Berg, A.; Wieland, M.; Doran, S.; Brochard, T.; Kamlowski, A.; Cellere, G.; Paccagnella, A.; Siegbahn, Erik A.; Prezado, Y.; Martinez-Rovira, I.; Bravin, A.; Dusseau, Laurent; and Berkvens, P.: Potential high resolution dosimeters for MRT 2010, 89-97.  
<https://ro.uow.edu.au/engpapers/4291>

Research Online is the open access institutional repository for the University of Wollongong. For further information contact the UOW Library: [research-pubs@uow.edu.au](mailto:research-pubs@uow.edu.au)

---

## Authors

E. Brauer-Krisch, Anatoly B. Rosenfeld, Michael L. Lerch, Marco Petasecca, M. Akselrod, J. Sykora, J. Bartz, M. Ptaszkiewicz, P. Olko, A. Berg, M. Wieland, S. Doran, T. Brochard, A. Kamlowski, G. Cellere, A. Paccagnella, Erik A. Siegbahn, Y. Prezado, I. Martinez-Rovira, A. Bravin, Laurent Dusseau, and P. Berkvens

# Potential High Resolution Dosimeters For MRT

E. Bräuer-Krisch<sup>\*</sup>, A. Rosenfeld<sup>#</sup>, M. Lerch<sup>#</sup>, M. Petasecca<sup>#</sup>, M. Akselrod<sup>†</sup>, J. Sykora<sup>†</sup>, J. Bartz<sup>†</sup>, M. Ptaszkiewicz<sup>‡</sup>, P. Olko<sup>‡</sup>, A. Berg<sup>‡</sup>, M. Wieland<sup>‡</sup>, S. Doran<sup>‡</sup>, T. Brochard<sup>\*</sup>, A. Kamlowski<sup>\*</sup>, G. Cellere<sup>‰,ℓ</sup>, A. Paccagnella<sup>‰</sup>, E. A. Siegbahn<sup>Ω</sup>, Y. Prezado<sup>\*</sup>, I. Martinez-Rovira<sup>\*,▲</sup>, A. Bravin<sup>\*</sup>, L. Dusseau<sup>¶</sup>, P. Berkvens<sup>\*</sup>

<sup>\*</sup>European Synchrotron Radiation Facility (ESRF), 6 rue Horowitz, BP220, F-38043 Grenoble, France

<sup>#</sup>Centre for Medical Radiation Physics, University of Wollongong, Wollongong, NSW2522, Australia

<sup>†</sup>Landauer, Inc., Stillwater Crystal Growth Division, Stillwater OK, 74074 USA

<sup>‡</sup>The Henryk Niewodniczanski Institute of Nuclear Physics Polish Academy of Sciences, Department of Radiation Physics and Dosimetry, ul. Radzikowskiego 152, PL 31-342 Krakow, Poland

<sup>‡</sup>Medizinische Universität Wien, Zentrum f. Biomedizinische Technik und Physik, Österreich

<sup>‡</sup>Department of Physics, University of Surrey, Guildford, UK

<sup>\*</sup>Bruker Biospin, Rheinstetten, Deutschland

<sup>‰</sup>DEI, Department of Information Engineering, via Gradenigo, 6/B, 35131 PADOVA, Italy

<sup>ℓ</sup>Applied Materials Baccini Via Postumia Ovest, 244, 31050 San Biagio di Callalta, Treviso

<sup>Ω</sup>Department of Medical Physics, Karolinska Universitetssjukhuset, 17176 Stockholm, Sweden

<sup>¶</sup>CEM<sup>2</sup>-Université MontpellierIIcc083, place E. Bataillon, 34095 Montpellier Cedex05 France

<sup>▲</sup>Institut de Tècniques Energètiques, Universitat Politècnica de Catalunya. Diagonal 647, E-08028 Barcelona (Spain)

**Abstract.** Microbeam Radiation Therapy (MRT) uses highly collimated, quasi-parallel arrays of X-ray microbeams of 50-600 keV, produced by 2<sup>nd</sup> and 3<sup>rd</sup> generation synchrotron sources, such as the National Synchrotron Light Source (NSLS) in the U.S., and the European Synchrotron Radiation Facility (ESRF) in France, respectively. High dose rates are necessary to deliver therapeutic doses in microscopic volumes, to avoid spreading of the microbeams by cardiosynchronous movement of the tissues. A small beam divergence and a filtered white beam spectrum in the energy range between 30 and 250 keV results in the advantage of steep dose gradients with a sharper penumbra than that produced in conventional radiotherapy. MRT research over the past 20 years has allowed a vast number of results from preclinical trials on different animal models, including mice, rats, piglets and rabbits. Microbeams in the range between 10 and 100 micron width show an unprecedented sparing of normal radiosensitive tissues as well as preferential damage to malignant tumor tissues. Typically, MRT uses arrays of narrow (~25-100 micron-wide) microplanar beams separated by wider (100-400 microns centre-to-centre, c-t-c) microplanar spaces. We note that thicker microbeams of 0.1-0.68 mm used by investigators at the NSLS are still called microbeams, although some investigators in the community prefer to call them minibeams. This report, however, limits its discussion to 25-100 µm microbeams. Peak entrance doses of several hundreds of Gy are surprisingly well tolerated by normal tissues. High resolution dosimetry has been developed over the last two decades, but typical dose ranges are adapted to dose delivery in conventional Radiation Therapy (RT). Spatial resolution in the sub-millimetric range has been achieved, which is currently required for quality assurance measurements in Gamma-knife RT. Most typical commercially available detectors are not suitable for MRT applications at a dose rate of 16000 Gy/s, micron resolution and a dose range over several orders of magnitude. This paper will give an overview of all dosimeters tested in the past at the ESRF with their advantages and drawbacks. These detectors comprise: Ionization chambers, Alanine Dosimeters, MOSFET detectors, Gafchromic<sup>®</sup> films, Radiochromic polymers, TLDs, Polymer gels, Fluorescent Nuclear Track Detectors (Al<sub>2</sub>O<sub>3</sub>:C, Mg single crystal detectors), OSL detectors and Floating Gate-based dosimetry system. The aim of such a comparison shall help with a decision on which of these approaches is most suitable for high resolution dose measurements in MRT. The principle of these detectors will be presented including a comparison for some dosimeters exposed with the same irradiation geometry, namely a 1×1 cm<sup>2</sup> field size with microbeam exposures at the surface, 0.1 cm and 1 cm in depth of a PMMA phantom. For these test exposures, the most relevant irradiation parameters for future clinical trials have been chosen: 50 micron FWHM and 400 micron c-t-c distance. The experimental data are compared with Monte Carlo calculations.

**Keywords:** Radiation Therapy, Dosimetry, Synchrotron Radiation, Gafchromic<sup>®</sup> film

## INTRODUCTION

Microbeam Radiation Therapy (MRT) is typically performed by using arrays of 20-100  $\mu\text{m}$  wide parallel beams, spatially fractionated by a centre-to-centre (c-t-c) distance of about 100-400  $\mu\text{m}$ , to irradiate a certain target although microbeams in the range of 0.1-0.68 mm thickness are still called microbeams by the NSLS investigators<sup>1,2</sup>. The clinical implementation of this therapy is best performed at a 3<sup>rd</sup> generation synchrotron facility with a negligible beam divergence and dose rates in the order of several thousands of Gy/sec to cope with the internal movements of the brain, due to the pulsation of the heart, which in the case of too slow exposures could lead to a blurring of the dose distribution produced by the microbeam array. The indispensable sharp slopes from the peaks to the valleys in the dose distribution can only be maintained if a) an adequate photon energy spectrum is used and b) a quasi parallel beam can be applied, which is the case for the ID17 biomedical beamline at the European Synchrotron Radiation Facility (ESRF) in Grenoble, France. The ratios between the peak and the valley doses (PVDRs) are believed to be of therapeutic importance and a maximum PVDR is radiobiologically desired, since the cells in the path of the dose peak will mainly be destroyed, while the valley dose must remain low enough for the normal tissue to be able to repair.

During the past decade, potential applications of Microbeam Radiation Therapy (MRT) have been studied experimentally at the National Synchrotron Light Source (NSLS) at Upton, New York, USA and at the ESRF<sup>1,3</sup>. Several references describe surprisingly high tissue tolerances to multiple microbeams, which is especially remarkable for developing tissues, well known to be radiosensitive<sup>4</sup>.

The rectangular microbeams (with typical size 25  $\mu\text{m} \times 0.5 \text{ mm}$ ) used in these experiments are produced when a multi-slit collimator intercepts the synchrotron beam. This beam is only 0.5 mm high but on the width of the beam there are fewer limitations. In order to irradiate a target with microbeams of a larger height (e.g. 1 cm instead of 0.5 mm), the irradiated object (e.g. phantom) is vertically translated in the beam during irradiation.

Absolute absorbed dose microdosimetry for dose values between 5 – 1000 Gy with the spatial resolution in the range of one micron still remains a challenge, since no commercial detector can be bought off shelf. Several approaches using MOSFET edge-on detectors<sup>5,6</sup> have proven to be useful, but were very time consuming and absolute dosimetry within  $\pm 3\%$  is currently not feasible. The spatially non-fractionated beam can be measured accurately enough by scanning

an ionization chamber through the beam or using Alanine dosimetry, but a reliable dosimetric on-line (real-time) system to measure PVDRs prior to patient irradiation needs to be developed to ensure perfect reproducibility when such microbeams are applied to treat patients. High spatial resolution in the measurement and reproducibility of the measured signal are particularly important. One potential candidate is a silicon strip detector system, currently under development.

## HIGH RESOLUTION DOSIMETERS

The choice of high resolution dosimeters has increased over the last years and in conventional radiation therapy the Gafchromic<sup>®</sup> films<sup>7,8</sup> are widely accepted to benchmark a TPS (Treatment Planning System) when high dose gradients need to be measured with submillimetric precision, like in the case of IMRT and radiation therapy treatment using the Gamma Knife. Measuring the absolute dose in the peak and in the valley in the case of MRT for clinical applications can currently only be covered by several approaches including cross-calibrations with ionization chambers in the spatially non-fractionated beam. Additionally, for most detectors, their energy dependence requires an additional correction, despite the fact that their mass attenuation coefficient may be very close to that of water (Figure 1) and in case of Si-based devices special care might be required due to the slight shift of the MRT energy spectrum from the peak to the valley<sup>6</sup>. The median energy for the filtered MRT spectrum is around 100 keV.

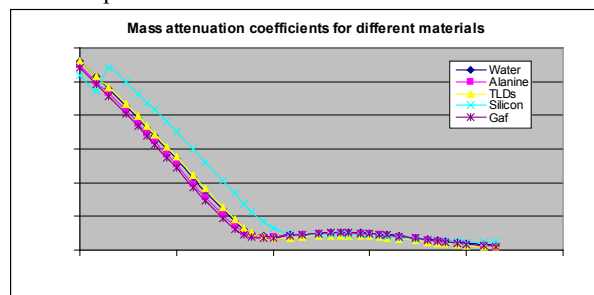


**FIGURE 1.** Comparison of mass attenuation coefficient of different materials typically used in dosimetry.

## FLASH MEMORY MOSFET

A Flash memory cell is a MOSFET where a polysilicon layer FG (Floating Gate) is interposed between the substrate and the control gate<sup>9</sup>. One can change the threshold voltage ( $V_{\text{TH}}$ ) of the MOSFET, thus permanently store a bit of information. Radiation will lead to charge losses from the programmed

floating gate<sup>10</sup>. The radiation-induced voltage shift can be translated into a dose information by appropriate physical models which take into account the effect of radiation source and energy spectrum<sup>11</sup>. Several devices were irradiated with a peak entrance dose of 100 Gy at the surface and submicron resolution can be achieved for the analysis of lateral dose profiles using these devices. The detector was exposed at the surface to a 10 x 10 mm<sup>2</sup> field. As a result a PVDR of 143 was measured for the 400 c-t-c case and 111 for the 200 c-t-c distance of the 25 μm wide microplanar beams. In this particular case, a comparison with Monte Carlo calculated PVDR is difficult, since these values are typically given in a depth between 0-10 mm and the PVDR changes rapidly with depth. From Siegbahn<sup>12</sup> we can extract a value of about 80 for similar parameters (10 x 10 mm<sup>2</sup>, 25 μm FWHM and 200 c-t-c distance) which compares rather well with the measured value of PVDR of 111 at the surface. These devices give submicron resolution, but a very unique readout device is required and absolute dosimetry would only be possible after careful energy calibration and necessary corrections to be applied for the energy shift from the different spectra in the peak and in the valley.

Also, in commercial devices, the analog information (VTH of the memory elements) is masked and only digital information (logical “0” or “1”) is available to the user. Hence, to obtain these results we had to use proprietary devices, equipments, and algorithms “instead of the user mode” routines of commercial devices.

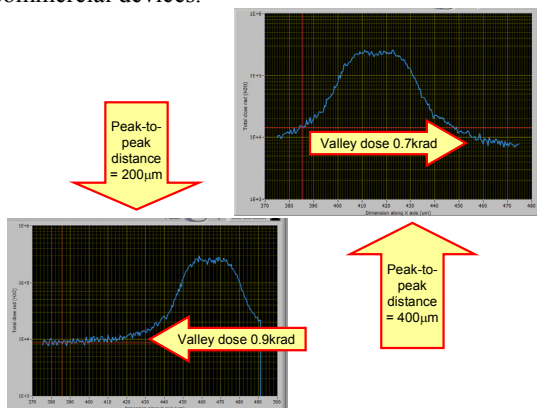


**FIGURE 2.** Example of dose deposition profiles of a microbeam using a Flash memory cell.

## MRI GEL DOSIMETRY

Polymer gel dosimetry is founded on the basis that monomers dissolved in the gel matrix polymerize due to the presence of free radicals produced by the radiolysis of water molecules. These radicals carrying

molecules represent the starting point for a polymerization process in the monomers, characterized by a double bond. The radical group is chemically very reactive and interacts with the double bond of the monomer. As a result the monomer will present an open binding (radical). The radical part of the monomer will interact with another monomer resulting in a dimer. The dimer again carries a radical, which is capable of catching the next monomer. The process will break off, when two radical carrying molecules meet each other. Polymer chains of different length are built up. The monomers and the surrounding water molecules are immobilized due to interaction with the corresponding interlaced polymer structure. The corresponding change in the autocorrelation time for motion results in a reduction of the transverse relaxation time T<sub>2</sub><sup>13,14</sup> in Magnetic Resonance (MR) due to less averaging of the dipolar magnetic interactions of the 1H-nuclear magnetic moments (Bloembergen-Purcell-Pound theory (BPP theory)). The parameter T<sub>2</sub> can be quantitatively mapped in 3 dimensions using Multi-Slice-Parameter selective MR-Imaging (MRI). The transverse relaxation time in many types of polymer gels linearly increases with dose within a limited dose range proposing the simple use of such polymer gels for relative dosimetry. At high dose levels and high dose rates usually a saturation regime is observed, which is characterized by increasingly less sensitivity. This region is assumed to be dominated by the consumption of monomers limiting the polymerization process. Even more important the reduction in the polymerization process may be dominated by the recombination of two radical carrying partners at high radical concentrations before finding a double bond partner within their pathway characterized by molecular diffusion.

MR-based Polymer gel dosimetry (MRPD) is characterized by tissue equivalence, 3D-data acquisition possibility by T<sub>2</sub>-multislice imaging and the capability for high spatial resolution, dependent on MRI equipment. The sensitivity regime and application range can be widely adjusted to the specific radiation characteristics, but is mainly limited up to now by its sensitivity to (high) dose rates as present in Synchrotron irradiation, and linear energy transfer. The accuracy is less than achievable by ionization chambers. Our preliminary test exposures have shown that MRPD especially designed for higher spatial resolution<sup>14,15</sup> is sensitive to the extraordinary high dose rates at several hundreds of Gy/s as present in MRT and thus offer yet unsatisfying results concerning dose response and spatial resolution.

## FLUORESCENT NUCLEAR TRACK DETECTOR (FNTD)

Fluorescent Nuclear Track Detectors is a new type of luminescent detectors for different applications in radiation dosimetry. They were originally developed for neutron and heavy charge particle dosimetry<sup>16</sup> and combine the advantages of solid state track detectors and optical measurements without the need for long chemical etching. The detectors are made of fluorescent aluminium oxide single crystals doped with carbon and magnesium ( $\text{Al}_2\text{O}_3:\text{C},\text{Mg}$ ) and are produced in different sizes and shapes depending on application. Thin, 500  $\mu\text{m}$ , polished wafers with diameter as large as 60 mm for radiation field imaging were recently produced. The tracks of recoil protons, heavy charge particles or overlapping tracks of photoelectrons and secondary ( $\delta$ ) electrons generated in single crystal aluminium oxide detector are imaged using high resolution readout system based on confocal laser scanning fluorescence microscopy technique<sup>16</sup>. Landauer currently is working on a compact table-top commercial instrument.

FNTDs were optimized for imaging applications over 4 orders of magnitude of photon doses<sup>17</sup> with dose range from 5 mGy to 50 Gy and extremely high spatial resolution of 0.6  $\mu\text{m}$ . High spatial resolution and wide dynamic range of dose measurements make FNTD technology very attractive for MRT quality assurance application when large peak-to-valley dose ratio has to be measured very precisely. FNTD is a passive integrating type of detector that does not require wires, electronics or batteries during irradiation. This detector is immune to electromagnetic interference and can measure doses at very high dose rate (was successfully tested at  $10^8$  Gy/s). FNTD detectors are made of sapphire and provide extremely good temperature and environmental stability, no light sensitivity, thermal fading or signal build-up. FNTD imaging plates are reusable after thermal annealing or optical bleaching.

PVDRs between 20-100 were measured for different parameters: 25, 50 and 75  $\mu\text{m}$  FWHM and 100, 200 or 400  $\mu\text{m}$  c-t-c spacing at 1, 11, 21 and 31 mm depth in a PMMA phantom for a field size of 10 x 10  $\text{mm}^2$ . Figure 3 depicts the results of imaging and processing of the microbeam field with 50  $\mu\text{m}$  FWHM and 400  $\mu\text{m}$  c-t-c spacing using a 4 x 6  $\text{mm}^2$  FNTD single crystal detector. The image of 1 x 4  $\text{mm}^2$  size was obtained in coarse scanning mode using 2D translation stages and the 3D plot was obtained in fine (1  $\mu\text{m}$ ) resolution mode using 2D galvanometer scanning. The images provide a detailed 3D dose distribution near the peak and in the valley of the beam. The cross-sections of the image for irradiated

and unirradiated detectors provide detailed information about PTVDR and low-dose detectability of FNTD technology.

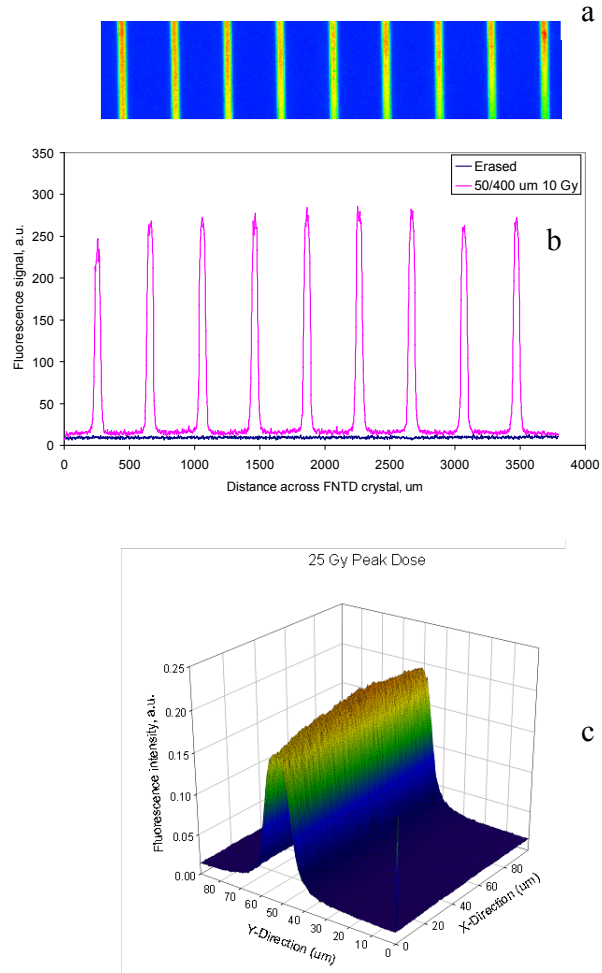


**FIGURE 3.** 3D dose mapping of 50/400  $\mu\text{m}$  microbeams using  $\text{Al}_2\text{O}_3:\text{C}, \text{Mg}$  crystals and FNTD technology: a) fluorescent image obtained by moving the detector with 2D translation stages; b) cross-section of the image (a) demonstrating the peak-to-valley dose ratio and comparison with erased detector background; c) 3D dose profile obtained with fine, 1  $\mu\text{m}$ , resolution galvanometer scanning.

## HIGH RESOLUTION TLD DOSIMETRY

The results of TLD dose measurements have been previously presented in a separate paper<sup>18</sup>. A two-dimensional (2-D) thermoluminescence (TL) dosimetry system consisting of  $\text{LiF}:\text{Mg},\text{Cu},\text{P}$  (MCP-N)-based TL foils and a TLD reader equipped with a CCD camera and the large size (72 mm in diameter) planchette heater was developed at the Institute of

Nuclear Physics to perform high resolution dosimetry. The TLDs were exposed to different microbeam

exposures where the results are listed in the Table 1 below.

**TABLE 1.** Comparison of the measured (right columns) and calculated (left columns) PVDRs; the differences in the measured value are from ~11-17% smaller than the Monte Carlo predicted values.

| FWHM (micron) | 25  | 50  | 75 | 25  | 50  | 75 |
|---------------|-----|-----|----|-----|-----|----|
| 200 c-t-c     | 107 | 56  | 29 | 95  | 48  | 24 |
| 400 c-t-c     | 224 | 119 | 62 | 191 | 105 | 54 |

In order to draw the right conclusions on high resolution measurements performed between 1996 and 2006, we have to keep in mind that the Monte Carlo calculations were simplified as follows: a) the source considered for the computed dose was a rectangular beam with perfectly parallel photons impinging on the target, typically a 16 cm diameter water phantom and b) the passage through the MSC was neglected in most of the publications until 2008 with the exception of H. Nettelbeck, who integrated some simplified source parameters and the geometry through the MSC<sup>19</sup>. This does lead to a decrease in the PVDR, which can well be the reason for the discrepancies measured in the past. This work is now in progress at the ESRF.

## GAFCHROMIC FILM DOSIMETRY

Due to the high dose rate and technical limitations, like the maximum possible goniometer speed of the motor used to scan the film through the spatially fractionated synchrotron radiation light, we are limited to a minimum peak dose of about 20 Gy. Within the range from 10-400 Gy, only the Gafchromic® films HD-810 from ISP (Nuclear Associates)<sup>7</sup> are adapted for our purposes.

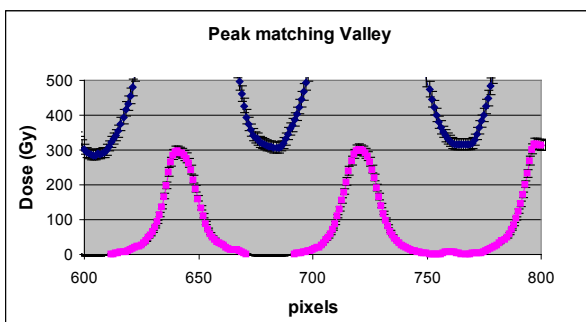


**FIGURE 4.** Two films exposed to doses which were corrected with a Monte Carlo pre-calculated dose ratio, in order to obtain similar valley and peak doses.

There are two possible choices to overcome the problem of the large dose range to be covered in MRT

dosimetry: 1) use 2 different sensitivities of Gafchromic® film as proposed by J. Crosbie<sup>20</sup> 2) apply a Monte Carlo pre-calculated PVDR to two separate exposures, one for the peak dose and one for the valley dose measurement, like in the example presented in Fig. 4.

As reported by Niroomand-Rad et al.<sup>8</sup> the orientation of the Gafchromic® film influences the measured optical densities. We have done a systematic analysis and observed that for homogenous exposures using linearly polarized Synchrotron Radiation, comparing the 90 degree rotated film with respect to the 0 degree irradiation direction, the maximum difference in optical densities for several series of MRT irradiated films is in the order of 10 % (10 x 10 mm<sup>2</sup> irradiation field).

To avoid these artefacts, related to the optical dichroism of the film, a standard convention for the exposure and readout procedure was established, with the thin coated side facing the beam: an “R” is marked on the upper right corner when looking downstream with the Synchrotron light (beams-eye-view) and the “R” is visible on the lower right corner when the film is positioned onto the glass plate of the Epson scanner V Pro 750, used to digitize the films. The optical density is then analyzed using the ImageJ software.

Before irradiation, the films are kept in their light tight black envelope and at room temperature (20 °C and never exceeding 25 °C). They are cut and prepared in a relatively dark room and kept in aluminium foil except during exposures. Because of the high dose rate at the ID17 beamline, the total exposure time to ambient light is never exceeding 5 minutes. The effect of this light has been described in different studies and our own tests showed no increase in optical density for films exposed less than 15 minutes at our typical light conditions. The readout of all films was done either with a JL (Joyce Loebel) microdensitometer or with an Epson scanner, not earlier than 2 days after the irradiation exposures, when the measured OD signal has reached a plateau. The resolution of the JL microdensitometer is superior to the Epson scanner and the results of this comparison will be published in a separate paper. On the other hand, the use of the microdensitometer is less reproducible and in a way

“user-dependant”, since the correct focus remains an individual adjustment of the apparatus influencing the pen deflection measuring the optical density. In figure 5 a typical scan using the JL microdensitometer is presented resulting in a measured PVDR of 66.7 for 50  $\mu\text{m}$  FWHM and 400 c-t-c at 10 mm depth. For the same parameters Monte Carlo calculations resulted in a PVDR of 65.

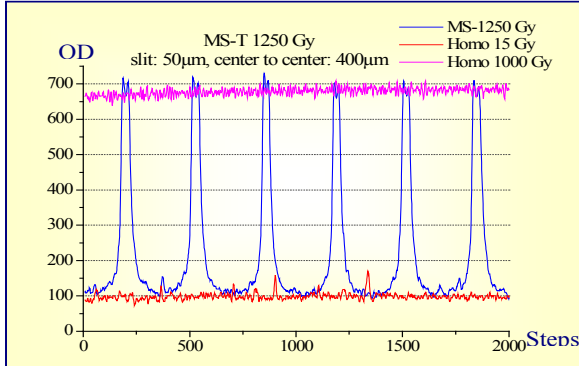


**FIGURE 5.** Relative OD of a microbeam exposed HD-810 film, measured by a JL microdensitometer. The solid lines correspond to a homogeneously exposed film of 15 Gy and 1000 Gy matching approximately the peak and the valley dose.

## OPTICAL COMPUTED TOMOGRAPHY WITH PRESAGE™ RADIOCHROMIC PLASTIC

Optical Computed Tomography (CT) works on much the same principle as x-ray CT, familiar from hospital medical imaging applications. In the case of 3-D dose mapping, the sample used is a radiochromic plastic named PRESAGE™. Being initially light yellow-green, the plastic colour changes locally to a dark green upon exposure to radiation. The degree of colour change (as quantified by the optical density) is proportional to the dose absorbed. The block of PRESAGE™ acts exactly like a “3-D film”. Readout is achieved using the optical Computed Tomography (CT) scanner described in Doran *et al.*<sup>21</sup> (Figure 6).

Research into using optical CT for MRT is still at an early stage, but it has been established that dosimetry in the dose range of tens to hundreds of Gy is achievable. Spatial resolution of around 20  $\mu\text{m}$  has been demonstrated and 50- $\mu\text{m}$  microbeams are easily visualized with the technique. Work is currently ongoing to determine the highest spatial resolution for which quantitative dosimetry data can be obtained. Previous studies have suggested that there is very little energy- or dose-rate dependence in the PRESAGE™

polymer’s response. Whilst it is known that the measured response is not stable in time (typical drifts are of order a few per cent per day), the response appears to remain linear with dose, so that all that is necessary is to create a dose-response calibration sample at the time the desired experiment is performed. Further studies are necessary to determine intra- and inter-batch reproducibility.

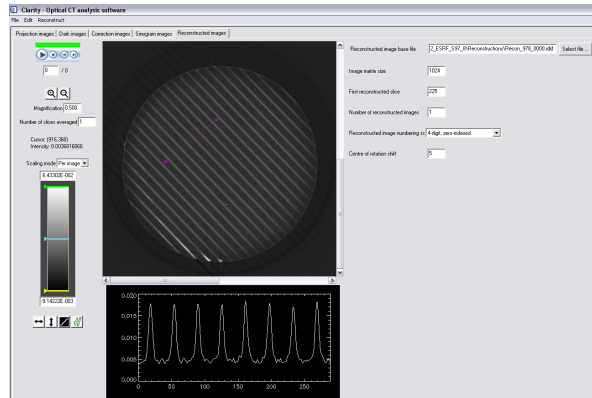


**FIGURE 6.** Example of a 2-D optical CT image from a sample at 9.7 mm depth (50  $\mu\text{m}$  FWHM, 400 micron c-t-c).

## SILICON STRIP DETECTOR DOSIMETRY

Radiation dosimetry in conformal radiotherapy using silicon diodes is well documented in the literature and is now well accepted in the clinical medical physics field as very useful tool. The physical parameters of the MRT beams, however, make it impossible to use such commercial silicon diodes for dosimetry in this case.

A silicon single strip detector and associated readout electronics has recently been tested at the ESRF. The new dosimetry system is designed to allow for very high spatial resolution measurements of the instantaneous dose rate at the detectors position in a phantom. The dose rate can then be integrated to estimate the total absorbed dose.

The dynamic range of the system is over five orders of magnitude, which makes it very suitable for MRT dosimetry. The spatial resolution (strip width) is 10  $\mu\text{m}$ . The energy dependence has been strongly improved due to the extremely small device dimensions, but this is of course still important, because compared to water, Si has a strong energy dependence for photons below 100 keV with its maximum at 50 keV.



The most important improvement is certainly the feature to either scan the single strip detector very fast across an array of microbeams up to 5 cm wide, or perform an on-line readout of the lateral microbeam profiles with high speed and high accuracy. These new devices allow a fast quality control of the microbeams just prior to a patient treatment at high enough resolution, currently not possible with any of the other dosimeters presented above.

The biggest drawback remains the improvement on adequate calibration and additional theoretical corrections required to measure absolute dose with these silicon detectors<sup>22</sup>. A high resolution scan as shown in figure 7 takes approximately 15 s.

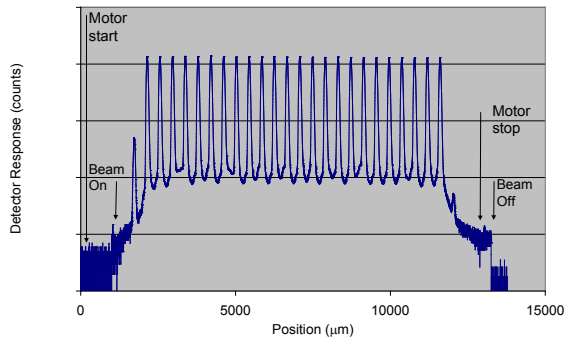


**FIGURE 7.** Fast silicon strip detector scan across an array of 25 microbeams.

## RESULTS AND CONCLUSIONS

Several high resolution dosimeters were presented in this paper, where most of them are still undergoing constant improvement and with respect to absolute dosimetry in MRT, further improvements are equally necessary in the Monte Carlo calculations in order to accurately benchmark in the future the calculated dose values with an accuracy of 3%. Currently several dosimeters are very promising and the different advantages and draw-backs are summarized in table 2 below.

Within the wide range of high resolution dosimeters presented here, each of them have some advantages and their individual limitations. Since the requirements in dosimetry for MRT are very demanding, at the present state there is no adequate single dosimeter available to measure the absolute dose accurately within 3% uncertainty. The Gafchromic<sup>®</sup> films represent a dosimeter with sufficient resolution, but their intrinsic fluctuation in the case of the HD-810 film type can be higher than

3%. Some of the dosimeters tested are inadequate, either due to their resolution or due to some dose rate effects. The important mission to benchmark a TPS in MRT must include several approaches to measure microdosimetric dose distributions in appropriate phantoms in order to increase the level of confidence. For the dose measurements of the spatially non fractionated beam, any dosimetry measurements should remain as much as possible to the standard protocols (IAEA TRS 386/389<sup>23</sup>), where ionization chambers are generally recommended. Whenever important additional corrections are required, like ion-recombination correction factors of more than 3%, a secondary standard like Alanine dosimetry should as well be done in combination with an adequate energy calibration, since these dosimeters are very well adapted for such high dose rates. The Gafchromic<sup>®</sup> film dosimetry is already used in the clinics, but in particular the resolution to be achieved strongly depends on the OD read-out system, where a JL microdensitometer is superior in terms of resolution, but more difficult to use than a high resolution commercial flatbed scanner. An additional disadvantage comes from the time dependence of the response of the dosimeter, which is only stable after about 24 hours, making dose verification just prior to a patient impossible. For this reason the Si-strip detector developed by the group of A. Rosenfeld at the CMRP University of Wollongong clearly shows the biggest advantage to measure on-line in a very fast, reliable and reproducible way with micron resolution the relative dose profiles. This feature makes such Si-strip detectors a prime candidate in terms of quality assurance when dose verification prior a possible MRT treatment is indispensable. The highest potential to measure absolute dose in the peak and in the valley in depth with high precision was demonstrated by the high resolution TLDs, the fluorescent Al<sub>2</sub>O<sub>3</sub> detectors developed by Landauer Inc., and the PRESAGE<sup>™</sup> read out with the optical computed tomography. The Gafchromic<sup>®</sup> film dosimetry remains an adequate tool where an overall precision within 8% can be achieved. Since none of these approaches will in the near future be an officially recognized prime standard, and most of them might even be not commercially available, further comparisons of these dosimeters should be perused until a good match is found between the improved Monte Carlo calculated dose and the measured value using different types of detectors.

**TABLE 2.** Comparison of different high resolution dosimeters tested in MRT. For completeness the ionization chamber and Alanine dosimeters are plotted in gray (suitable dosimeters for the homogenous field measurements only).

| Detector type  | Advantage/<br>Limitations                             | Dose<br>range                                     | Spatial<br>resolution      | Energy<br>dependence                | Dose rate<br>dependence                            | Stability in<br>time                          | Reproducibility                                |
|--|---|---|----------------------------|-------------------------------------|--|---|--|
| PRESAGE™<br>+opt. CT<br>(S.Doran)  | Not<br>commercial                                     | 10-500 Gy   | 20 µm                      | To be<br>investigated               | To be<br>investigated                              | To be<br>investigated                         | 3%   |
| Si Strip (A.<br>Rosenfeld/ M.<br>Lerch)  | Special device<br>for MRT<br>specific needs           | 10 Gy-<br>50000 Gy                                | 10 µm                      | Strong, to<br>be corrected          | To be<br>investigated                              | 5% /year                                      | Better than 2%                                 |
| OSL (L.<br>Dusseau)  | CCD readout<br>difficult                              |   | <100<br>micron             | Nearly<br>tissue<br>equivalent      | To be<br>investigated                              | Good  | Good   |
| Gafchromic (HD-<br>810 (J. Crosbie,<br>E. Bräuer-Krisch)   | “Easy”<br>evaluation,<br>commercial                   | 10-400 Gy   | 12.5 µm<br>(µdensitometer) | Nearly<br>tissue<br>equivalent      | Apparently<br>none                                 | Very bad<br>(<24 hours)<br>afterwards<br>O.K. | 3-8%   |
| Alanine (A.<br>Kamlowski)  | High dose   | 200 Gy-<br>200 kGy<br>(F)<br>1 Gy -200<br>kGy (P) | ~1 mm                      | Strong, to<br>be corrected          | None up to<br>1000 kGy                             | Very good                                     | 0.5%   |
| Ionization<br>chamber (ESRF)   | IAEA TRS<br>398<br>recommended                        | 18/51<br>kGy/min<br>(standard/<br>weblene)        | > mm                       | Yes, but<br>small                   | Yes, ion<br>recombination<br>corrections<br>needed | Very good                                     | 0.1-1%   |
| TLDs (high<br>resolution)<br>(P.Olko)  | Often<br>secondary<br>Standard                        | 0.01-500<br>Gy                                    | ~ 5 µm                     | Can be<br>corrected                 | Not investigated                                   | Fading  | 1-3%   |
| Polymer gels (A.<br>Berg)  | Tissue<br>equivalence,<br>3D/Dose rate<br>sensitivity | 0.01 to<br>100 Gy                                 | > 100 µm                   | No<br>dependence<br>(0.1-20<br>MeV) | Strong above<br>5 Gy/min                           | Bad   | 1.5-4.5% for low<br>dose rates                 |
| Fluorescent<br>Nuclear Track<br>Detectors<br>(Al <sub>2</sub> O <sub>3</sub> :C,Mg)<br>(M. Akselrod,<br>Landauer Inc.) | Soon to be<br>commercially<br>available               | 0.005-50<br>Gy                                    | 0.6 µm                     | Over<br>response of<br>2 vs. water  | None, up to 10 <sup>8</sup><br>Gy/s                | Very good<br>temperature<br>time<br>stability | Very good for<br>gamma, to be<br>tested for SR |
| Floating gate<br>based Dosimetry<br>(G. Cellere)   | Not<br>commercial<br>devices and<br>readout modes     | 0.01-100<br>Gy                                    | < 1 µm                     | Strong                              | none   | Very good                                     | Good   |

## ACKNOWLEDGMENT

The authors would like to thank the entire team of the ID17 biomedical beamline for their valuable help and support and all those who have tried over the years to solve this tricky problem.

## REFERENCES

<sup>1</sup> D.J. Ansel, P. Romanelli, H. Benveniste et al., *Minim Invas Neurosurg* **50**, 43 (2007).

<sup>2</sup> F. A. Dilmanian, P. Romanelli, N. Zhong et al., *European Journal of Radiology* **68S** S129–S136 (2008).  
<sup>3</sup> D. N. Slatkin, P. Spanne, F. A. Dilmanian et al., *Proc Natl Acad Sci U S A* **92** (19), 8783 (1995); J. A. Laissue, N. Lyubimova, H. P. Wagner et al., presented at the Proc. Of SPIE, Denver, USA, 1999 (unpublished); J. A. Laissue, G. Geiser, P. O. Spanne et al., *Int J Cancer* **78** (5), 654 (1998); F. A. Dilmanian, T. M. Button, G. Le Duc et al., *Neuro-oncol* **4** (1), 26 (2002); F. A. Dilmanian, G. M. Morris, N. Zhong et al., *Radiat Res* **159** (5), 632 (2003); N. Zhong, G. M. Morris, T. Bacarian et al., *Radiat Res* **160** (2), 133 (2003); F. A. Dilmanian, Y. Qu, S. Liu et al., *Nucl Instrum Methods Phys Res A* **548** (1-2), 30 (2005); F. A. Dilmanian, Y. Qu, L. E. Feinendegen et al., *Exp Hematol* **35** (4 Suppl

- 1), 69 (2007); F. A. Dilmanian, Z. Zhong, T. Bacarian et al., *Proc Natl Acad Sci U S A* **103** (25), 9709 (2006); M. Miura, H. Blattmann, E. Bräuer-Krisch et al., *Br J Radiol* **79** (937), 71 (2006); H. M. Smilowitz, H. Blattmann, E. Bräuer-Krisch et al., *J Neurooncol* **78** (2), 135 (2006).
- 4 J. A. Laissue, H. Blattmann, D. Michiel et al., presented at the Proc. of SPIE, Washington, 2001 (unpublished); H. Blattmann, W. Burkard, V. Djonov et al., *Strahlenther. Onkol* **178**, 118 (2002); F. A. Dilmanian, G. M. Morris, G. Le Duc et al., *Cell Mol Biol* **47** (3), 485 (2001).
- 5 E. Bräuer-Krisch, A. Bravin, M. Lerch et al., *Med Phys* **30** (4), 583 (2003); A. Rosenfeld, E. A. Siegbahn, E. Brauer-Krisch et al., *IEEE Trans. Nucl. Sci.* **52**, 2562 (2005).
- 6 E. A. Siegbahn, E. Brauer-Krisch, A. Bravin et al., *Med Phys* **36** (4), 1128 (2009).
- 7 ISP, (2007); ISP, (2008).
- 8 A. Niroomand-Rad, *Medical Physics American Association of Physicists in Medicine Med. Phys* (25), 2093–115 (1998).
- 9 P. Cappelletti, Kluwer Academic Publishers: New York (2000).
- 10 G. Cellere and A. Paccagnella, *IEEE Transaction on Device and Material Reliability*, **3** (4), 359 (2004).
- 11 G. Cellere, A. Paccagnella, A. Visconti et al., *IEEE Trans. on Nucl. Sci.* **54** (4), 1066 – 1070 (2007).
- 12 E Siegbahn, A., J Stepanek, E. Bräuer-Krisch et al., *Med. Phys.* **33** (9), 3248 (2006).
- 13 M.J. Maryanski, J.C. Gore, R.P. Kennan et al., *Magn. Reson. Imaging* **11**, 253–258 (1993).
- 14 Y. De Deene, C. Hurley, K. Venning et al., *Phys. Med. Biol.* **47**, 3441–3463 (2002).
- 15 C. Bayreder, D. Georg, E. Moser et al., *Med. Phys.* **33** (7), 2506 (2006).
- 16 G.M. Akselrod, M.S. Akselrod, E.R. Benton et al., *NIM B* **247** (247), 296 (2006).
- 17 G.J. Sykora and M.S. Akselrod, *Rad. Meas.*, in press (2010).
- 18 M. Ptaszkiwicz, E. Bräuer-Krisch, M. Klosowski et al., *Radiation Measurements* **43**, 990 (2008).
- 19 H. Nettelbeck, G. J. Takacs, M. L. Lerch et al., *Med Phys* **36** (2), 447 (2009).
- 20 J. C. Crosbie, I. Svalbe, S. M. Midgley et al., *Phys Med Biol* **53** (23), 6861 (2008).
- 21 S. Doran, T. Brochard, J. Adamovics et al., *Phys Med Biol* **55** 1531–1547 (2010).
- 22 M. Lerch, H. Nettelbeck, H. Requardt et al., 10th International Conf. on Synchrotron Radiation Instrumentation, September, Melb. 2009 (2009).
- 23 P.) IAEA (Andreo, IAEA **TRS398** (2004).